FLOW AROUND AND HEAT AND MASS TRANSFER OF A SPHERE WITH BLOWING AT MEDIUM REYNOLDS NUMBERS

M. V. Bashkatov and S. I. Shabanov

UDC 532.516:532.526:536.24

The Navier–Stokes and heat- and mass-transfer equations are solved numerically for a sphere with uniform blowing over the surface in the Reynolds number range up to 20. A method of refining the boundary conditions far from the sphere is proposed in both problems. A difference scheme from other authors is used to solve the hydrodynamic problem, and an explicit difference scheme with a second order of approximation is used for the heat problem. It is shown that blowing diminishes the aerodynamic drag of the sphere and the temperature or concentration gradient at its surface, i.e., the heat- and mass-transfer intensity.

Analytic solutions of the problems of the flow around and of the heat and mass transfer of a sphere with uniform blowing on the surface at Reynolds and Péclet numbers less than one have been obtained in [1, 2] by the method of uniting asymptotic expansions.

This paper proposes to obtain the solution of the same problem, but by numerical methods and for values of the Re* criterion up to 20, which is of interest for certain high-speed processes, for example, for the plasmochemical reprocessing of atomized materials (here Re = $2aU_\infty\upsilon^{-1}$; a is the radius of the sphere, U_∞ is the free-stream velocity, and υ is the coefficient of kinematic viscosity).

It is considered that the injected gas has the same constants as the free gas stream, and no chemical or phase transformations occur in the neighborhoods of the sphere. The influence of nonisothermy is assumed slight; hence, first the independent solution of the hydrodynamic problem in an isothermal flow is admissible and then of the thermal problem.

The streamline problem reduces to solving the Navier–Stokes and continuity equations, which can be expressed in dimensionless form in terms of the stream function ψ and the vortex $\xi = \operatorname{rot} V$ as follows;

$$D^2\psi = \xi r \sin\theta;$$

$$\frac{\mathrm{Re}^*}{2}\left[\frac{\partial\psi}{\partial r}\frac{\partial}{\partial\theta}\left(\frac{\xi}{r\sin\theta}\right) - \frac{\partial\psi}{\partial\theta}\cdot\frac{\partial}{\partial r}\left(\frac{\xi}{r\sin\theta}\right)\right]\sin\theta = D^2(\xi r\sin\theta),$$

where $D^2 = \frac{\partial^2}{\partial r^2} + \frac{\sin\theta}{r^2}\cdot\frac{\partial}{\partial\theta}\left(\frac{1}{\sin\theta}\cdot\frac{\partial}{\partial\theta}\right)$ is the Stokes operator, $r = \bar{r}/a$ is the dimensionless radius, $\theta = \pi$ is the free-stream direction. Hence

$$V_r = -\frac{\partial\psi}{\partial\theta}\Big/r^2\sin\theta, \quad V_\theta = \frac{\partial\psi}{\partial r}\Big/r\sin\theta,$$

where V_r and V_θ are the dimensionless radial and tangential stream velocity components.

The boundary conditions on the surface are the following for a sphere with blowing: $V_r = k$, $V_\theta = 0$ for r = 1 or

$$\psi = -k(1-\cos\theta); \quad \xi = \frac{\partial^2\psi}{\partial r^2}\Big/\sin\theta, \tag{1}$$

Novosibirsk. Translated from Zhurnal Priladnoi Mekhaniki i Tekhnicheskoi Fiziki, No. 4, pp. 148-156, July-August, 1975. Original article submitted January 23, 1975.

where $k=V_1/U_\infty$ is the blowing parameter, and V_1 is the radial blowing velocity on the sphere surface.

The relationships

$$\text{for } \theta=0 \quad V_\theta=0; \quad \partial V_r/\partial\theta=0; \quad \psi=0; \quad \xi=0;$$
$$\text{for } \theta=\pi \quad V_\theta=0; \quad \partial V_r/\partial\theta=0; \quad \psi=-2k; \quad \xi=0.$$

are valid on the axis of symmetry.

Unperturbed stream conditions are usually used as boundary conditions at an infinite distance from the sphere.

There is apparently a unique numerical cosolution of the hydrodynamic problem for a sphere with blowing under the same assumptions in [3]. From that paper, the explicit difference scheme was borrowed to compute the velocities at all points of the field, which must be known in order to solve the thermal problem. However, a refinement was introduced into the methodology of the solution.

The fact is that it is impossible to give $r\to\infty$ in the numerical computations. Hence, it was assumed in [3] that the unperturbed stream conditions already hold on a finite, although significant, radius A. Such a hypothesis assumes the selection of A quite large, which increases the number of mesh nodes and the volume of the calculations needed.

To eliminate the disadvantages mentioned, it is proposed to use the analytical solution for the Oseen domain obtained in [1] as the boundary conditions on a finite radius A:

$$\psi=\frac{A^2\sin\theta}{2}-k(1-\cos\theta)+\frac{4B}{\mathrm{Re}^{*2}}(1-\cos\theta)\left\{1-\exp\left[-\frac{A\,\mathrm{Re}^*}{4}(1+\cos\theta)\right]\right\};$$
$$\xi=\frac{B}{2A}\left(1+\frac{4}{A\,\mathrm{Re}^*}\right)\sin\theta\exp\left[-\frac{A\,\mathrm{Re}^*}{4}(1+\cos\theta)\right]. \tag{2}$$

Here B is a factor which was found in [1] by merging the expressions (2) with the solutions for the space near the sphere.

It is admissible to consider that the same character of the flow is conserved for medium Reynolds numbers far from the sphere where the perturbations are weakened significantly, i.e., the boundary conditions on the radius A express (2) to the accuracy of the coefficient B.

The values of B can be found by using the known integral relation

$$F_i=-\int_\Omega [L_i(V_jn_j)-\Pi_{ij}]\,d\Omega, \tag{3}$$

where F_i is the aerodynamic drag, L_i is the i-th component of the momentum, V_j, n_j are, respectively, the j-th component of the velocity and the normal to Ω , and π_{ij} is the stress tensor.

Substituting (2) into (3) and integrating over an infinitely remote surface yields

$$B=(k+C_f/8)\,\mathrm{Re}^{*2}/4,$$

where $C_f=(C_1+C_2)$ is the aerodynamic drag coefficient of a sphere with blowing defined by numerical integration of the friction (C_1) and pressure (C_2) forces over the sphere surface. The corresponding components were calculated by means of the equations

$$C_1=\frac{8}{\mathrm{Re}^*}\int_0^\pi \xi\sin^2\theta\,d\theta; \quad C_2=4\int_0^\pi p\sin\theta\cos\theta\,d\theta, \tag{4}$$

where the pressure p was determined for each θ by means of the vortex distribution law found over the surface of the sphere,

$$p = p_{\theta=0} + 1/2 \int_0^\theta \left\{ \frac{2}{\mathrm{Re}^*} \left[\left(\frac{\partial \xi}{\partial r} \right) + \xi \right] - k\xi \right\}_{r=1} d\theta.$$

After the velocity field has been determined, the thermal problem is solved, i.e., the heat-balance equation, in the following dimensionless form:

$$\frac{1}{r^2} \frac{\partial}{\partial r} \left(r^2 \frac{\partial h}{\partial r} \right) + \frac{1}{r^2 \sin\theta} \cdot \frac{\partial}{\partial \theta} \left(\sin\theta \frac{\partial h}{\partial \theta} \right) = \frac{\mathrm{Pe}}{2} \left(V_r \frac{\partial h}{\partial r} + \frac{V_\theta}{r} \frac{\partial h}{\partial \theta} \right). \tag{5}$$

Here $h = (T - T_\infty)/(T_a - T_\infty)$ is the dimensionless temperature (or concentration) T_a is the sphere surface temperature, T_∞ is the free-stream temperature, $\mathrm{Pe} = 2aU_\infty/D$; and D is the temperature conduction coefficient.

The boundary conditions of the sphere surface are h = 1 for r = 1; h = 0 as $r \to \infty$ in the unperturbed flow; and on the axis of symmetry

$$dh/d\theta = 0. \tag{6}$$

As in the flow problem, the radius is measured in the logarithmic scale Z = ln r and (5) goes over into the following:

$$\frac{\partial^2 h}{\partial Z^2} + \frac{\partial h}{\partial Z} + \frac{\partial^2 h}{\partial \theta^2} + \mathrm{ctg}\,\theta \cdot \frac{\partial h}{\partial \theta} = \frac{\mathrm{Pe}}{2} \left(V_Z \frac{\partial h}{\partial Z} + V_\theta \frac{\partial h}{\partial \theta} \right) \exp Z. \tag{7}$$

As in the previous case, the analytical solution obtained in [2] for this domain for small values of the Reynolds and Péclet numbers is used as the boundary conditions on a large, but finite radius A:

$$h = \frac{B_1}{r} \exp\left[-\frac{\mathrm{Pe}}{4} r (1 + \cos\theta) \right]. \tag{8}$$

The coefficient B_1 can be found by using the integral relation

$$\int_{\Omega_2} \left(\frac{\mathrm{Pe}}{2} V_r h - \frac{\partial h}{\partial r} \right)_{r=A} d\Omega_2 - \int_{\Omega_1} \left(\frac{\mathrm{Pe}}{2} V_r h - \frac{dh}{\partial r} \right)_{r=1} d\Omega_1 = 0, \tag{9}$$

which reflects the fact that the enthalpy flux through a spherical surface Ω_2 with radius A in a gas volume without sources in a steady-state mode is equal to its flux standing off from the solid surface of a sphere Ω_1.

Substituting conditions (1), (6), and (8) into (9) and taking the unperturbed flux condition $V_r \approx -\cos\theta$, in a first approximation on the radius A, we obtain

$$\int_0^{2\pi} \int_0^{\pi} \left\{ -\frac{B_1 \mathrm{Pe}}{2r} \cos\theta \exp\left[-\frac{\mathrm{Pe}}{4} r (1 + \cos\theta) \right] - \frac{\partial}{\partial r} \left(\frac{B_1}{r} \times \right.\right.$$
$$\left.\left. \times \exp\left[-\frac{\mathrm{Pe}}{4} r (1 + \cos\theta) \right] \right) \right\}_{r \to \infty} r^2 \sin\theta \, d\theta d\varphi - \int_0^{2\pi} \int_0^{\pi} \left(\frac{\mathrm{Pe}\,k}{2r} - \frac{\partial h}{\partial r} \right)_{r=1} \times$$
$$\times \sin\theta d\theta d\varphi = 2\pi (2B_1 - \mathrm{Pe}\,k - \mathrm{Nu}) = 0.$$

Therefore

$$B_1 = \frac{\mathrm{Pe}\,k + \mathrm{Nu}}{2}, \quad \text{where } \mathrm{Nu} = -\int_0^\pi \left(\frac{\partial h}{\partial r} \right)_{r=1} \sin\theta d\theta. \tag{10}$$

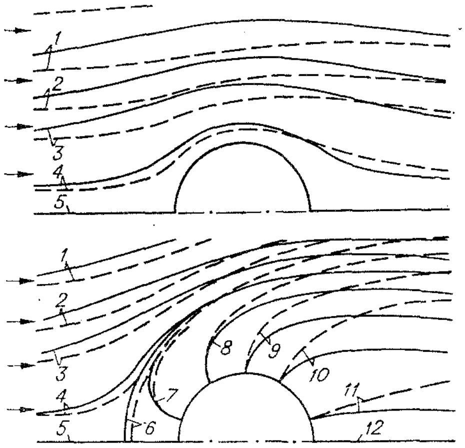

Fig. 1

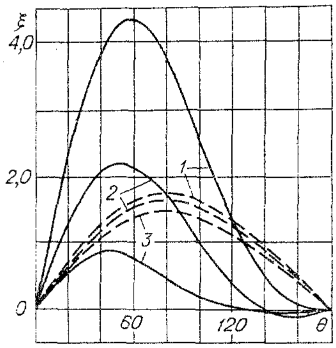

Fig. 2

The expression (8) with the value of B_1 from (10) was taken as a more exact boundary condition on the radius A, where the Nusselt criterion (Nu) was found by numerical integration over the sphere surface and was refined in each interaction.

The hydrodynamic and thermal problems were solved numerically by using the same mesh. An explicit difference scheme with a second-order approximation, analogous to that used in the hydrodynamic problem, was used for the thermal problem. If the magnitude of the spacing and its number in the $Z = \ln r$ direction are denoted by ζ and i, and in the angle θ by ϑ and j, then the difference equation becomes

$$h[i+1,j]\left[\frac{4+\zeta(2-\mathrm{Pe}\,V_Z[i,j]\exp Z[i])}{4\zeta^2}\right]+$$
$$+h[i-1,j]\left[\frac{4-\zeta(2-\mathrm{Pe}\,V_Z[i,j]\exp Z[i])}{4\zeta^2}\right]+$$
$$+h[i,j+1]\left[\frac{4+\vartheta(2\operatorname{ctg}\theta[j]-\mathrm{Pe}\,V_Z[i,j]\exp Z[i])}{4\vartheta^2}\right]+$$
$$+h[i,j-1]\left[\frac{4-\vartheta(2\operatorname{ctg}\theta[j]-\mathrm{Pe}\,V_Z[i,j]\exp Z[i])}{4\vartheta^2}\right]-h[i,j]\left[\frac{2}{\zeta^2}-\frac{2}{\vartheta^2}\right]=0.$$

Taking account of (6), Eq. (7) for the axis of symmetry for both $\theta = 0$ and $\theta = \pi$ becomes, after the indeterminacy therein has been resolved,

$$\frac{\partial^2 h}{\partial Z^2}+\frac{\partial h}{\partial Z}+2\frac{\partial^2 h}{\partial \theta^2}=\frac{\mathrm{Pe}}{2}V_Z\frac{\partial h}{\partial Z}\exp Z.$$

Having expressed the increment h by using a Taylor series, the boundary condition on the axis of symmetry can be represented with a second-order approximation as follows for $\theta = 0$:

$$h[i,0]\left(1+\frac{\vartheta^2}{2\zeta^2}\right)-h[i,1]-h[i+1,0]\{4+\zeta(2-$$
$$-\mathrm{Pe}\,V_Z[i,0]\exp Z[i])\}\frac{\vartheta^2}{16\zeta^2}-h[i-1,0]\{4-\zeta(2-$$
$$-\mathrm{Pe}\,V_Z[i,0]\exp Z[i])\}\frac{\vartheta^2}{16\zeta^2}=0.$$

For $\theta = \pi$, when $j = m$, the equation has the same form but with the subscript j replaced by m instead of zero, and by $m - 1$ instead of 1.

TABLE 1

Parameters	κ	Re*					
		1	5	10	15	20	1 from [1]
C_1		18,366	4,741	2,823	2,118	1,739	19,0
C_2	0	9,134	2,402	1,482	1,142	0,954	9,5
C_f		27,500	7,143	4,305	3,260	2,693	28,5
C_1		17,715	4,137	2,225	1,529	1,160	18,4
C_2	0,2	9,051	2,391	1,500	1,187	1,028	9,4
C_f		26,766	6,528	3,725	2,717	2,188	27,8
C_1		17,130	3,601	1,745	1,098	0,772	17,8
C_2	0,4	8,978	2,363	1,503	1,212	1,071	9,3
C_f		26,108	5,964	3,248	2,310	1,843	27,1
C_1		16,560	3,132	1,369	0,795	0,527	17,2
C_2	0,6	8,915	2,333	1,495	1,223	1,093	9,2
C_f		25,475	5,465	2,864	2,018	1,620	26,4
C_1		16,007	2,722	1,080	0,589	0,378	16,6
C_2	0,8	8,831	2,303	1,484	1,224	1,102	9,1
C_f		24,838	5,025	2,564	1,813	1,480	25,7
C_1		15,471	2,370	0,862	0,452	0,287	16,0
C_2	1,0	8,758	2,269	1,469	1,224	1,103	9,0
C_f		24,229	4,639	2,331	1,676	1,390	25,0

The numerical solution of all the equations was carried out by using an electronic computer. The mesh spacing ϑ in the angle θ was 6°, and $\zeta=0.1$, was selected in Z = ln r, where it was assumed that $\ln A=3$ ($A\approx 20$). Values of Re* and k were given, and the hydrodynamic problem was solved first. For k = 0, the known Stokes solution was taken as the initial approximation and ψ and ξ were refined by iterations. Each solution obtained was used to determine the initial approximation for the next value of k by means of relations resulting from [1]

$$\psi_n \approx \psi_{n-1} - (k_{n-1} - k_n)(1 - \cos\theta),\ \xi_n \approx \xi_{n-1}.$$

The selection of the iteration parameter for each value of Re* was carried out in conformity with [4]. The difference schemes were solved by the Zeidel' method [5]. Refinement of ψ, ξ and h, as well as of C_f and Nu, terminated when the difference between the values of the first three functions became less than 10^{-4} in successive iterations.

After the velocity field has been determined for given Re* and k, the solution of the thermal problem was repeated for six values of the Prandtl criterion S = ν/D in 0.1 steps, starting from 0.5 and going to 1.

The temperature field in a fixed medium when h = 0 on the radius A

$$h = \frac{1}{A-1}\left(\frac{A}{r} - 1\right)$$

was taken as the initial approximation at k = 0.

The temperature field found was taken as the initial approximation for the next k. The blowing parameter k was varied between 0 and 1 in 0.2 steps in the inner cycle, and

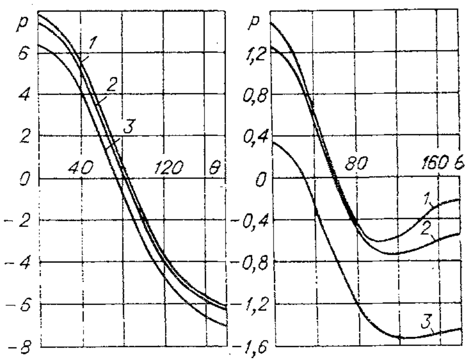

Fig. 3

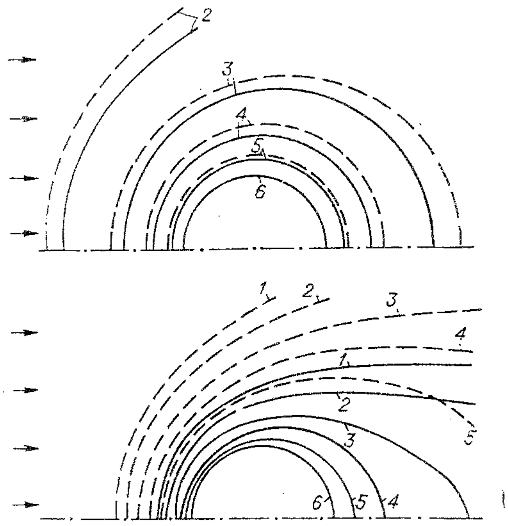

Fig. 4

Re* took the values 1, 5, 10, 15, and 20 in the outer cycle.

Shown at the top in Fig. 1 are the streamlines for k = 0, and below for k = 1 for Re* = 1 (solid lines) and Re* = 20 (dashes); the ψ correspond to curves 1-5 for the values ψ = 2, 1, 0.5, 0.05; 0 and the values $\psi = 0, -0.05, -0.5, -1, -1.5, -1.95$, and -2 correspond to the curves 6-12. Comparing the graphs shows how strongly blowing deforms the velocity field by forcing the free stream from the solid surface to the streamline $\psi = 0$.

Figure 2 illustrates the vortex distribution over the surface of the sphere for Re* = 1 (dashes) and Re* = 20 (solid lines), where k = 0, 0.4, and 1 correspond to curves 1-3. Figure 2, in which the same notation is used, shows the pressure distribution over the sphere surface (Re* = 1 on the left and Re* = 20 on the right).

The aerodynamic drag coefficient of a sphere with blowing as a function of Re* and k is shown in Table 1. Given in the last column are values calculated on the basis of the analytical solution [1]:

$$C_1 = \frac{16}{\mathrm{Re}^*}\left(1 + \frac{3}{16}\mathrm{Re}^* - \frac{3k}{16}\mathrm{Re}^*\right); \tag{11}$$

$$C_2 = \frac{8}{\mathrm{Re}^*}\left(1 + \frac{3}{16}\mathrm{Re}^* - \frac{k}{16}\mathrm{Re}^*\right). \tag{12}$$

The good agreement between the results in the first and last columns indicates the satisfactory accuracy of the numerical solution and the possibility of using (11) and (12) up to Re* = 1.

It follows from (4) and (11) that C_1 diminishes for all values of Re* as k grows. Physically this is explained by the reduction of the velocity gradient at the sphere surface (Fig. 1) and the diminution in the vorticity (Fig. 2). For small Re* the component C_2 also diminishes as k grows since the pressure on the frontal hemisphere is hence reduced more than on the root. However, for large Re* the forcing back of the free stream by the blowing substance is so great that restoration of the pressure behind the root is considerably worse. Hence, as Fig. 3 shows, as k grows the pressure on the frontal hemisphere is reduced, although less than at the root, and the component C_2 grows. Nevertheless, the growth of C_2 still is small in the region investigated and is cancelled completely by the reduction in C_1, whereupon the quantity C_f decreases monotonically as k increases.

Exhibited in Fig. 4 is the temperature field around the sphere in the case S = 1 for Re* = 1 (upper) and Re* = 20 (lower) for k = 0 (solid lines) and k = 1 (dashes). Curves 2-6 refer to the values of h between 0.2 and 1.0 in 0.2 steps, and curve 1 to the value h = 0.1.

It is seen that similarly to the streamlines, the isotherms are also "forced back"

TABLE 2

S	k	Re* 1	Re* 5	Re* 10	Re* 15	Re* 20	k	Re* 1	Re* 5	Re* 10	Re* 15	Re* 20
0,5		2,148	2,666	3,100	3,438	3,725		2,076	1,977	1,730	1,477	1,242
0,6		2,174	2,730	3,214	3,583	3,893		2,046	1,901	1,617	1,333	1,079
0,7	0	2,200	2,811	3,325	3,716	4,044	0,6	2,019	1,845	1,518	1,204	0,936
0,8		2,229	2,883	3,425	3,836	4,181		2,008	1,795	1,423	1,085	0,812
0,9		2,256	2,950	3,517	3,947	4,306		2,004	1,745	1,332	0,976	0,704
1,0		2,282	3,012	3,595	4,050	4,422		2,000	1,695	1,252	0,378	0,611
0,5		2,133	2,460	2,596	2,674	2,709		2,032	1,766	1,382	1,050	0,782
0,6		2,125	2,437	2,595	2,666	2,688		1,995	1,667	1,240	0,888	0,621
0,7	0,2	2,136	2,457	2,613	2,666	2,668	0,8	1,964	1,586	1,115	0,750	0,493
0,8		2,152	2,480	2,622	2,656	2,640		1,948	1,511	1,001	0,632	0,390
0,9		2,168	2,499	2,625	2,641	2,606		1,926	1,440	0,897	0,533	0,309
1,0		2,184	2,515	2,627	2,621	2,569		1,919	1,370	0,800	0,448	0,245
0,5		2,109	2,202	2,135	2,017	1,879		1,997	1,572	1,088	0,725	0,471
0,6		2,083	2,156	2,067	1,922	1,758		1,945	1,453	0,932	0,568	0,337
0,7	0,4	2,075	2,135	2,011	1,834	1,645	1,0	1,907	1,352	0,798	0,444	0,240
0,8		2,079	2,117	1,956	1,749	1,536		1,876	1,260	0,682	0,347	0,170
0,9		2,085	2,097	1,901	1,664	1,432		1,851	1,173	0,582	0,270	0,120
1,0		2,091	2,076	1,846	1,581	1,334		1,829	1,091	0,496	0,210	0,086

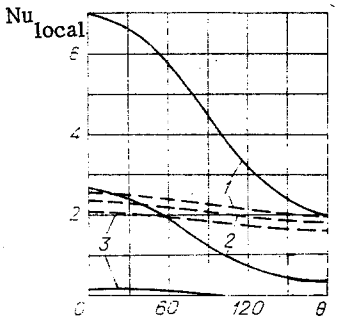

Fig. 5

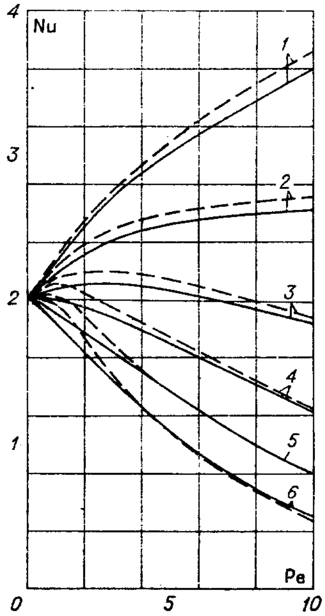

Fig. 6

from the sphere, whereupon the temperature or concentration gradient diminishes, especially at the root. The local Nusselt criteria, whose distribution along the sphere surface is shown in Fig. 5, also diminish correspondingly (here S = 1, the dashed lines refer to Re* = 1, the solid lines to Re* = 20, and k = 0, 0.4, and 1.0 correspond to curves 1-3).

The average values of the Nusselt criterion (10) also diminish with the increase in k, as is seen from Fig. 6 where its change as a function of Pe is shown for S = 0.5 (dashes) and S = 1.0 (solid lines). Values of k between 0 and 1.0 in 0.2 steps correspond to curves 1-6. In the coordinates taken Nu depends comparatively weakly on the Prandtl criterion, at least for large Pe and k. In Nu–Re* coordinates, the dependence on S is stronger, as can be traced from the Table 2 in which more detailed and exact values about the dependence of the average Nu on Re*, k, and S are presented.

LITERATURE CITED

1. M. V. Bashkatov and S. I. Shabanov, "Flow around a sphere with a transverse stream of substance at low Reynolds numbers, " Zh. Prikl. Mekh. Tekh. Fiz., No. 3 (1972).
2. M. V. Bashkatov and S. I. Shabanov, "Heat transfer of a sphere with blowing in a slow flow," Zh. Prikl. Mekh. Tekh. Fiz., No. 4 (1972).
3. A. E. Hamielec, T. W. Hoffman, and L. L. Ross, "Numerical solutions of the Navier–Stokes equation for flow past spheres, Pt. 1, AIChE. J. 13, No. 2 (1967).
4. B. P. LeClair, A. E. Hamielec, and H. R. Pruppacher, "A numerical study of the drag on a sphere at low and intermediate Reynolds numbers," J. Atmos. Sci. 27, No. 2 (1970).
5. I. S. Berezin and N. P. Zhidkov, Calculation Methods [in Russian], Vol. 2, Fizmatgiz, Moscow (1962).